English
Research Express@NCKU Volume 14 Issue 5 - June 18, 2010
[http://research.ncku.edu.tw/re/articles/e/20100618/3.html]

Nitride-Based MSM Photodetectors with a HEMT Structure and a Low-Temperature AlGaN Intermediate Layer

Ricky W. Chuang[1,*], K. H. Lee[1], P. C. Chang[2], and S. J. Chang[1]

[1] Institute of Microelectronics, Department of Electrical Engineering, Center for Micro/Nano Science and Technology, and Advanced Optoelectronic Technology Center, National Cheng Kung University
[2] Department of Electronic Engineering, Nan Jeon Institute of Technology

rwchuang@mail.ncku.edu.tw

Journal of The Electrochemical Society, 2008, Vol. 155(12), H959-H963

AlGaN/GaN high electron mobility transistor (HEMT) is a widely studied structure for applications in high power and high frequency electronic devices. The unique characteristics of AlGaN/GaN heterostructural devices typically involve the current transport via the two-dimensional electron gas (2DEG) and a modulation field applied in a direction parallel with the heterointerface. High density carriers in the channel as confined by barriers could render promising properties that are potentially useful for numerous device applications such as HEMT, photodetectors (PDs), and other devices with special functionalities. Introducing a 2DEG layer into the metal-semiconductor-metal (MSM) PD structure has two attractive features. First, the electric field within the device structure can be modified in a way of improving the device performance compared to other conventional MSM PDs. Secondly, fabrication processes of both PD and HEMT are compatible with each other that they could be prepared jointly in one single epitaxial growth. Unfortunately, the resultant epitaxial quality of these devices is often compromised by the presence of threading dislocations (TD) in the GaN epitaxial films due to a large lattice mismatch between GaN and sapphire substrate. In order to enhance the interfacial quality of AlGaN/GaN heterostructure, a low-temperature (LT) grown AlGaN intermediate layer is proposed as an intermediate layer between the two high-temperature (HT) grown GaN layers before growing the final AlGaN/GaN epitaxial layers. In this way the resultant crystalline quality of AlGaN/GaN heterostructures could be substantially improved as the TDs at the interface is effectively thwarted from propagating into the active device regions. Incorporation of a LT-grown layer between HT grown GaN layers has been reported by Iwaya *et al*. [1] as a way to limit the defects propagation. The TDs near the island edge are prone to bending due to the presence of the image force, prompting the dislocation lines to extend with a much faster rate in a lateral growth direction. This bending leads to a defect-free material in the region between islands. In this study, the characterizations of high quality AlGaN/GaN epitaxial layers with LT AlGaN intermediate layer inserted in between HT grown GaN layers are first reported. Ultraviolet (UV) MSM PDs based on AlGaN/GaN heterostructure with and without a LT AlGaN intermediate layer are fabricated and characterized thereafter in detail.

All samples studied in this paper were all grown using metalorganic chemical vapor deposition (MOCVD). Sapphire (0001) was used as the substrate. Trimethyl-aluminum (TMAl), trimethyl-gallium (TMGa) and ammonia (NH_3) were used as group III and V source gases, respectively. Immediately after subjecting sapphire substrate to a thermal annealing treatment with hydrogen flowing in an enclosed chamber at 1120°C, the graphite susceptor was then cooled down to 600°C in order to deposit 30 nm LT GaN buffer layer. HT-GaN was then grown at 1050°C over the LT buffer layer. The thickness of the first HT-GaN layer was kept at 1.75 μm. Then, the LT $Al_{0.3}Ga_{0.7}N$ intermediate layer with thickness of 100 nm was deposited at 500°C, followed by the deposition of second 0.25 μm HT-GaN layer and 20 nm $Al_{0.25}Ga_{0.75}N$ layer (epi-structure for PD_A). The deposition conditions invoked for the first and second HT-GaN layer growth were identical. In comparison, 2 μm HT-GaN layer and 20 nm $Al_{0.25}Ga_{0.75}N$ layer without including the LT $Al_{0.3}Ga_{0.7}N$ intermediate layer were also deposited on the LT buffer layer (epi-structure for PD_B).

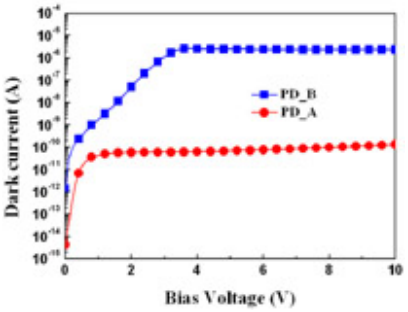

Fig. 1. Dark current-voltage characteristics of both fabricated MSM PDs.

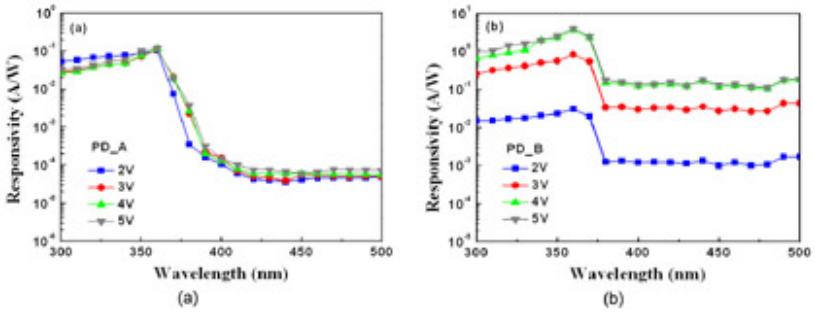

Fig. 2. Spectral responses at different bias of (a) PD_A and (b) PD_B.

Figure 1 shows room temperature dark current-voltage characteristics of PD_A and PD_B without and with AlGaN/GaN HEMT structure, respectively. The magnitude of the dark current generated by this device structure is mainly contributed by the cathode depletion region that shares the largest part of the applied voltage. Here, we define V_p as the bias voltage at which the 2DEG channel below the cathode depletion region is being pinched off. Figure 2 shows the device spectral responsivity measured with various applied biases. A sharp cutoff around the absorption band edge of GaN (i.e., 360 nm) is observed from both PDs. Under the illumination of xenon light source with an incident light wavelength of 360 nm at room temperature, as bias voltage is increased from 2V to 5V, the responsivities thus measured varied from 0.11 to 0.12 A/W for PD_A, but a larger fluctuation range varied from 0.03 to 4.08 A/W is observed instead for PD_B. Figure 3 depicts the measured responsivities at 360 nm as a function of applied reverse bias for both PDs. It was found that the measured responsivity was almost bias-independent for PD_A, while a steep increase in responsivity was observed for PD_B. In addition, the measured responsivity at voltage above 1 V was abnormally large for PD_B. Such a result suggested that a larger internal gain in fact existed in PD_B.

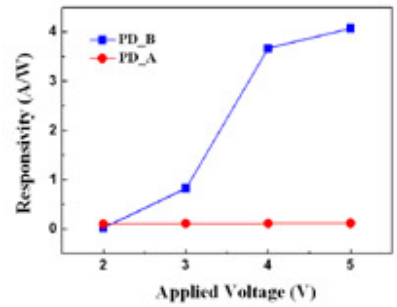

Fig. 3. Measured responsivity at 360 nm as a function of applied bias for both PDs.

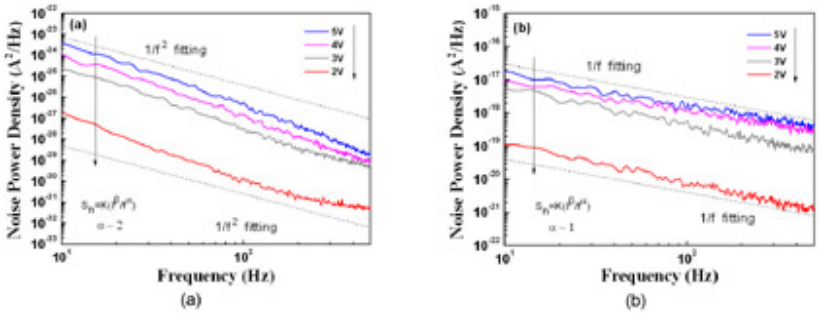

Fig. 4. Noise power spectra of (a) PD_A and (b) PD_B.

Figure 4(a) and (b) shows noise power spectra of the PD_A and PD_B gathered by applying different biases. As shown in Fig. 4, it is found that α is close to 2 for PD_A and 1 for PD_B throughout the measured frequency range. In other words, the low frequency noise is dominated by $1/f$-type noise in PD_A, as compared to $1/f^2$-type noise domination in PD_B. The insets of Figs. 5(a) and 5(b) show the noise power density of our devices as a function of dark current measured at 100 Hz. The β value was estimated to be 2 for both PD_A and PD_B. Knowing the values of α and β, and with data shown in Fig. 4, the K value can be determined from $S_n(f) = K(I^\beta/f^\alpha)$ to be 1.16×10^{-7} for PD_A and 2.09×10^{-7} for PD_B, where I is the dark current, f is the frequency, K is a constant, and α and β are two fitting parameters. As presented in Fig. 5(a), the noise equivalent power (*NEP*) increases while the normalized detectivity (D^*) decreases monotonically with the applied bias, and this is because the rate of increase in responsivity is comparably much slower compared to that of the total noise current power as applied bias is increased for PD_A. Thus, it can be suggested that *NEP* and D^* of PD_A are both dominated by the total noise current power. On the other

hand, as shown in Fig. 5(b), an opposite trend for PD_B is observed instead when compared with PD_A; that is, *NEP* decreases and *D*∗ increases with the applied bias. As already depicted in Fig. 5, the internal gain is directly responsible for the abnormally large responsivity obtained from PD_B, and what contributed to this internal gain was most likely due to the unwanted noises generated within the device, which were evidently related to interfacial defects of the device under study. Without an extra LT AlGaN intermediate layer included for PD_B, the presence of interfacial defects is expected to contribute to the unusually large responsivity as the applied bias is increased. Therefore, it is reasonable to suggest that both *NEP* and *D*∗ of PD_B are dominated by the fluctuation in responsivity. With a 5 V applied bias, *NEP* and *D*∗ measured for PD_A were 2.65×10^{-10} W and 1.74×10^{9} cmHz$^{0.5}$W^{-1}, respectively. At the same bias, *NEP* and *D*∗ for PD_B were 1.62×10^{-8} W and 2.85×10^{7} cmHz$^{0.5}$W^{-1}, respectively. The resultant detectivity (*D*∗) of PD_A is noticeably better compared with other previously reported AlGaN-based MSM or Schottky barrier PDs [2-3]. These findings indicate that a lower noise level and a larger detectivity can be realized by introducing an additional LT AlGaN intermediate layer into the buffer multilayer structure.

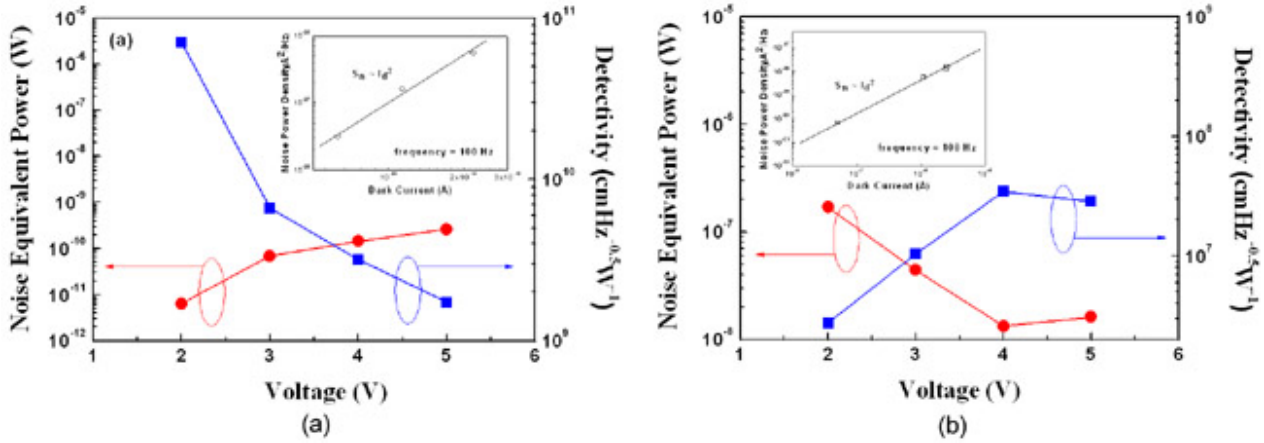

Fig. 5. Noise equivalent power (*NEP*) and normalized detectivity (*D**) of (a) PD_A and (b) PD_B. Insets show the corresponding noise power density measured at 100 Hz.

In summary, UV MSM PDs based on AlGaN/GaN HEMT structure with LT AlGaN intermediate layer were successfully fabricated. These particular PDs are compatible with the HEMT fabrication process (i.e., allowing a direct monolithic integration with HEMT-based circuits in one epitaxial step) due to their simple planar structure. The subsequent measurement results concluded that a reduction in the dark leakage current and a simultaneous enhancement in gate controllability could in fact be achieved when compared to the conventional PDs. For the PDs with the LT AlGaN intermediate layer, the responsivity at 360 nm and UV/visible rejection were respectively obtained as 0.12 A/W and 10^{3} at the bias voltage of 5 V. Finally, with the same applied bias, the *NEP* and *D** of these very devices obtained were 2.65×10^{-10} W and 1.74×10^{9} cmHz$^{0.5}$W^{-1}, respectively.

References

[1] M. Iwaya, T. Takeuchi, S. Yamaguchi, C. Wetzel, H. Amano, and I. Akasaki, Jpn. J. Appl. Phys. **37**, L 316 (1998).
[2] D. Walker, X. Zhang, A. Saxler, P. Kung, J. Xu, and M. Razeghi, Appl. Phys. Lett. **70**, 949 (1997).
[3] E. Monroy, F. Calle, E. Muñoz, F. Omnès, P. Gibart, and J. A. Muñoz, Appl. Phys. Lett. **73**, 2146 (1998).